



# Benchmarking an operational procedure for rapid risk assessment in Europe

**Francesco Dottori, Milan Kalas, Peter Salamon, Alessandra Bianchi, Lorenzo Alfieri, Luc Feyen**

European Commission, Joint Research Centre, Directorate for Space, Security and Migration, Via E. Fermi 2749, 21027 Ispra, Italy.

francesco.dottori@jrc.ec.europa.eu

**Keywords:** real-time, early warning system, flood hazard mapping, flood impact, economic damage, risk assessment

## *Abstract*

The development of methods for rapid flood mapping and risk assessment is a key step to increase the usefulness of flood early warning systems, and is crucial for effective emergency response and flood impact mitigation. Currently, flood early warning systems rarely include real-time components to assess potential impacts generated by forecasted flood events. To overcome this limitation, this work describes the benchmarking of an operational procedure for rapid flood risk assessment based on predictions issued by the European Flood Awareness System (EFAS). Daily streamflow forecasts produced for major European river networks are translated into event-based flood hazard maps using a large map catalogue derived from high-resolution hydrodynamic simulations. Flood hazard maps are then combined with exposure and vulnerability information, and the impacts of the forecasted flood events are evaluated in terms of flood prone areas, economic damage and affected population, infrastructures and cities.

An extensive testing of the operational procedure is carried out by analysing the catastrophic floods of May 2014 in Bosnia-Herzegovina, Croatia and Serbia. The reliability of the flood mapping methodology is tested against satellite-based and report-based flood extent data, while ground-based estimations of economic damage and affected population are compared against modelled estimates. Finally, we evaluate the skill of risk estimates derived from EFAS flood forecasts with different lead times and combinations of probabilistic forecasts. Results show the potential of the real-time operational procedure in helping emergency response and management.

## *1) Introduction*

Nowadays, flood early warning systems (EWS) have become key components of flood management strategies in many rivers (Cloke et al., 2013; Alfieri et al., 2014a). They can increase



37 preparedness of authorities and population, thus helping reduce negative impacts (Pappenberger  
38 et al., 2015). Early warning is particularly important for cross-border river basins where  
39 cooperation between authorities of different countries may require more time to inform and  
40 coordinate actions (Thielen et al., 2009).

41 In this context, the European Commission has developed the European Flood Awareness System  
42 (EFAS) which provides operational flood predictions in major European rivers as part of the  
43 Copernicus Emergency Management Services. The service is fully operational since 2012 and  
44 available to hydro-meteorological services with responsibility in flood warning, EU civil  
45 protection and their network.

46 While early warning systems are routinely used to predict flood magnitude, there is still a gap in  
47 the ability to translate flood forecasts into risk forecasts, that is, to evaluate the possible impacts  
48 generated by forecasted events (e.g. flood prone areas, affected population, flood damages losses).  
49 Currently, flood impacts are generally evaluated considering static flood scenarios, either related  
50 to official maps issued by the competent authorities (EC 2007) or to synthetic events derived from  
51 current or future climatology (Alfieri et al., 2015), which implies some degree of manual  
52 interpretation of forecasts to delineate flood prone areas and define impacts. A few research  
53 projects are being developed where flood impact estimation is automated and linked to event  
54 forecasting (Rossi et al., 2015; Schulz et al., 2015; Saint-Martin et al., 2016), however to our  
55 knowledge these systems are still at experimental phase, and not yet integrated into operational  
56 EWS.

57 Indeed, the availability of real-time operational systems for assessing potential consequences of  
58 forecasted events would be a substantial advance in helping emergency response, and indeed  
59 flood impact forecasts are increasingly being requested by end users of early warning systems  
60 (Emerton et al., 2016; Ward et al., 2016). At local scale, impact forecasting may provide valuable  
61 information to alert local civil protection services and plan measures to increase preparedness, for  
62 instance monitoring and strengthening flood defences and planning evacuation measures. At  
63 European scale, the possibility to receive prior information on expected flood impacts would  
64 increase preparedness and response time of the Emergency Response Coordination Centre  
65 (ERCC), in order to plan and coordinate support for national emergency services.

66 In the present paper, we describe a methodology designed to meet the needs of EWS users and  
67 overcome the limitations mentioned so far. The methodology translates EFAS flood forecasts into  
68 event-based flood hazard maps, and combines hazard, exposure and vulnerability information to  
69 produce risk estimations in near-real time. All the components are fully integrated within the  
70 EFAS forecasting system, thus providing seamless risk forecasts at European scale.

71 To demonstrate the reliability of the proposed methodology, we perform a detailed assessment  
72 focused on the 2014 floods in the Sava River Basin in Southeast Europe. A large dataset for the  
73 evaluation and validation of the results has been collected, which consists of observed flood  
74 magnitude, flood extent derived from different satellite imagery datasets, and detailed post-event  
75 evaluation of flood impacts, economic damage assessment and affected population and  
76 infrastructure.



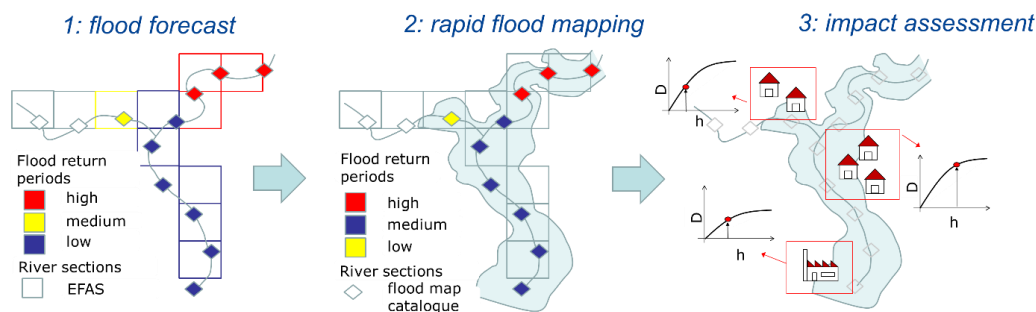
77 The reliability of the flood mapping procedure is first assessed by assuming a “perfect” forecast,  
78 where flood magnitude is taken from real observations instead of EFAS predictions. The effect  
79 of flood defences failure is also taken into account. After that, we test the performance of the  
80 operational flood forecasting procedure, to evaluate the influence of different lead times and  
81 combination of forecast members.

## 82 2) Methodology

83

84 In this section we describe the three components which compose the rapid risk assessment  
85 procedure: 1) streamflow and flood forecasting; 2) event-based rapid flood mapping 3) impact  
86 assessment. Figure 1 shows a conceptual scheme of the step composing the methodology.

87



88

89 *Figure 1: conceptual scheme of the rapid risk assessment procedure*

90

91 The basic workflow of the procedure is the following:

- 92 • Every time a flood event is forecasted, we identify the river sections affected and local flood  
93 magnitude, (expressed as return period of the peak discharge);
- 94 • we identify areas which might be flooded using a the map catalogue, which contains all the  
95 flood prone areas for each river section and flood magnitude; these local flood maps are then  
96 combined to derive event-based hazard maps;
- 97 • Event hazard maps are combined with exposure information to assess affected population,  
98 infrastructures and urban areas, and economic damage.

99

100 The following sections provide a detailed description of each component.

101

### 102 2.1 The European Flood Awareness System (EFAS)

103

104 The European Flood Awareness System (EFAS) produces streamflow forecasts for Europe using  
105 a hydrological model driven by daily weather forecasts. We provide here a general description of  
106 the EFAS components, the reader is referred to the website ([www.efas.eu](http://www.efas.eu)) and to published



107 literature for further details (Thielen et al., 2009; Pappenberger et al., 2011; Cloke et al., 2013;  
108 Alfieri et al., 2014a).

109 Hydrological simulations in EFAS are performed with Lisflood (Burek et al., 2013; van der Knijff  
110 et al., 2010), a distributed physically based rainfall-runoff model combined with a routing module  
111 for river channels. The model is calibrated at European scale using streamflow data from a large  
112 number of river gauges and meteorological fields interpolated from point measurements of  
113 precipitation and temperature. Based on this calibration, a reference hydrological simulation for  
114 the period 1990–2013 is run for the European window at 5 km grid spacing, and updated daily.  
115 This reference simulation provides initial conditions for daily forecast runs of the Lisflood model  
116 driven by the latest weather predictions, which are provided twice per day with lead times up to  
117 10 days. To evaluate the magnitude of streamflow forecasts in every grid point of the simulation  
118 domain, these are compared with local discharge thresholds, statistically evaluated from the  
119 reference simulation (Alfieri et al., 2014a). In case thresholds are exceeded persistently over  
120 several forecasts, flood warnings for the affected locations are issued to the members of the EFAS  
121 consortium.

122 To account for the inherent uncertainty of the weather forecast, EFAS adopts a multi-model  
123 ensemble approach, running the hydrological model with forecasts provided by the European  
124 Centre for Medium Weather Forecast (ECMWF), the Consortium for Small-scale Modelling  
125 (COSMO), and the Deutscher Wetterdienst (DWD),

## 126 *2.2 Database of flood hazard maps*

127

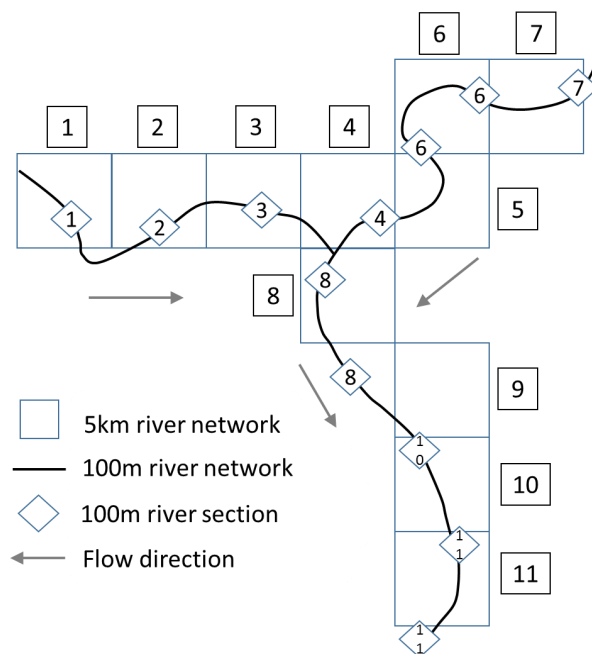
128 Linking streamflow forecast with inundation mapping is complex because inundation modelling  
129 tools are computationally much more demanding than hydrological models used in early warning  
130 systems, which currently prevent a real time integration of these two components. To overcome  
131 this limitation, in the present work we decided create a catalogue of flood inundation maps  
132 covering all the EFAS river network and linked to EFAS streamflow forecast.

133 The hydrological input for creating the map catalogue is derived from the stream flow dataset of  
134 the EFAS reference simulation, described in Section 2.1. The information is available on the  
135 EFAS river network at 5 km grid spacing for rivers with upstream drainage areas larger than 500  
136 km<sup>2</sup>. The streamflow data is downscaled to a high-resolution river network (100m), where  
137 reference sections are identified at regular spacing along stream-wise direction each 5km. Figure  
138 2 shows a conceptual scheme of the two river networks. For each of these reference sections, a  
139 statistical analysis of extreme value analysis is applied to derive discharge values for several  
140 reference return periods (10, 20, 50, 100, 200 and 500 years), which are then combined with flow  
141 duration curves to produce flood hydrographs (see Alfieri et al., 2014b for a detailed description).  
142 The hydrographs are used to run flood simulations at 100 m resolution in each river section using  
143 the 2D hydrodynamic model LISFLOOD-FP (Bates et al., 2010).

144 The 100m flood maps related to the same EFAS river section (i.e. pixel of the 5km river network)  
145 are merged together, to identify the areas at risk of flooding because of overflowing from a



146 specific EFAS river section, and archived in the flood map catalogue. The merging is performed  
147 separately for each return period, in order to relate flooded areas with the magnitude of the flood  
148 event.



149  
150 *Figure 2: conceptual scheme of the EFAS river network (5 km, squares) with the high resolution*  
151 *network (100m) and river sections (diamonds) where flood simulations are derived. The sections*  
152 *of the two networks related are indicated by the same number. Adapted from Dottori et al. (2015).*  
153

### 154 2.3 Event-based mapping of flood hazard

155

156 The database of flood hazard maps described in Section 2.2 is used to translate the information  
157 coming from EFAS discharge forecasts into event-based estimations of flood extent. Since the  
158 EFAS daily predictions are provided as an ensemble of forecasts, the procedure to identify flood  
159 prone areas and flood magnitude is also carried out in a probabilistic framework.

160 We first identify the maximum discharge predicted over the full forecasting period, calculated  
161 using the median discharge from ensemble forecasts at each river grid cell. The value is compared  
162 with the reference long-term climatology to calculate the return period.

163 Then, predicted streamflow is compared with the local flood protection level, and river grid cells  
164 where the protection level is exceeded are considered to activate the complete risk assessment  
165 procedure.

166 Flood protection levels are given as the return period of the maximum flood event which can be  
167 retained by the defence measures (e.g. dykes). The map of flood protections used is based on risk-



168 based estimations for Europe developed by Jongman et al. (2014), integrated, where available,  
169 with the actual level of protection found from literature review or assessed by local authorities.  
170 Selected river cells are reclassified into classes according to the closest return period exceeded  
171 (10, 20, 50, 100, 200, 500 years) and the corresponding flood hazard maps are retrieved from the  
172 catalogue and tiled together. For instance, if the estimated return period is 40 years, the flood map  
173 for 20 years return period is used. Where more maps related to more river sections overlap (see  
174 Section 2.2), the maximum depth value is taken.

#### 175 *2.4 Flood impact and risk assessment*

176

177 After the event-based flood hazard map has been completed, it is combined with the available  
178 information defining the exposure and vulnerability at European scale.

179 The number of people affected is calculated using the population map developed by Batista e  
180 Silva et al. (2012) at 100m resolution. A detailed database of infrastructures produced by Marín  
181 Herrera et al. (2015) is used to compute the extension of the road network affected during the  
182 flood event. The list of major towns and cities potentially affected within the region is derived  
183 from an internally developed map of major urban areas. The total extension of urban and built-up  
184 areas (differentiated between residential, commercial and industrial areas) and agricultural areas  
185 is computed using the latest update of the Corine Land Cover for the year 2006.

186 The land use layer is also used as asset exposure information to compute direct economic losses  
187 in combination with flood hazard variables (flood extent and depths) and depth-damage functions,  
188 following the approach applied by Jongman et al. (2012), Rojas et al. (2013) and Alfieri et al.  
189 (2015). The set of empirical damage functions derived for European countries by Huizinga (2007)  
190 have been elaborated to produce separate functions for the land use classes that are more  
191 vulnerable to flooding (residential, commercial, industrial, agricultural). To account for the  
192 variable value of assets within one country, damage values are corrected considering the ratio  
193 between the gross domestic product (GDP) of regions (identified according to the Nomenclature  
194 of Territorial Units for Statistics (NUTS), administrative level 1) and country's GDP. To enable  
195 the application of the methodology in all the EFAS domain, additional damage curves have been  
196 derived for countries not included in the original database, like Serbia and Bosnia-Herzegovina.  
197 All the results computed during the risk assessment procedure are aggregated using the  
198 classification of EU regions of EUMetNet (the network of European Meteorological Services,  
199 www.meteoalarm.eu). The regions considered are based on the levels 1 and 2 of the NUTS  
200 classification, according to the EU country, with the advantage of providing areas of aggregation  
201 with a comparable extent.

202 In the operational system, the described procedure is fully integrated in the EFAS forecast  
203 analysis chain. When a new EFAS hydrological forecast becomes available, the risk assessment  
204 procedure is activated in those locations where predicted peak discharges exceeds the flood  
205 protection levels. When activated, the execution time depends on the extent and spatial spread of  
206 the potentially affected areas over the full forecasting domain. Even in case of flood events



207 occurring simultaneously in different European countries, the results of the analysis are delivered  
208 within one hour after the EFAS forecast runs are finished.

### 209 ***3) Benchmarking of the procedure***

210

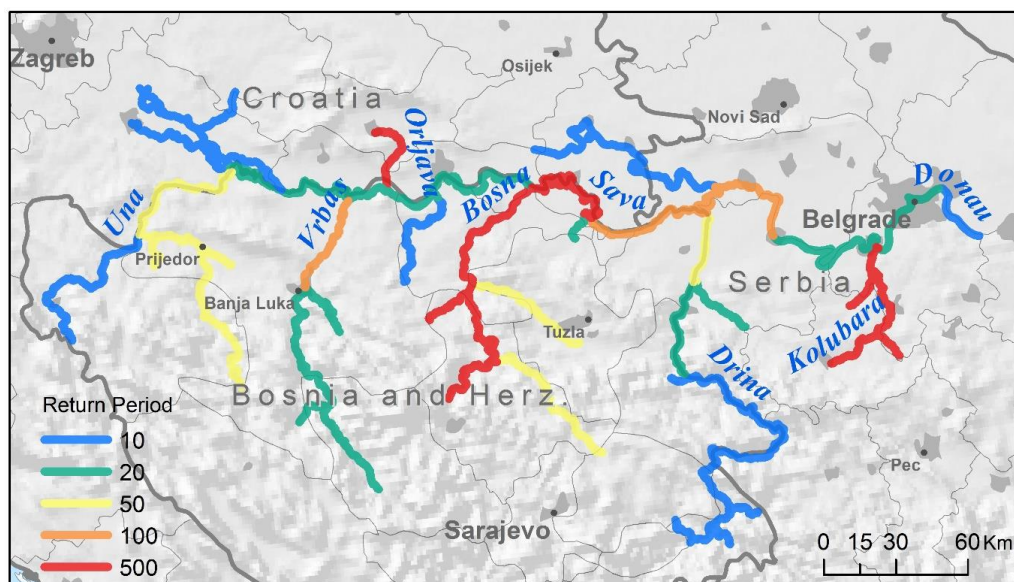
211 In order to perform a comprehensive evaluation of the risk assessment procedure, it is important  
212 to evaluate each component of the methodology, namely, streamflow forecasts, event-based flood  
213 mapping, and the impact assessment. The skill of EFAS streamflow forecasts is routinely  
214 evaluated (Pappenberger et al., 2011) while impact assessment was successfully applied by  
215 Alfieri et al. (2016) to evaluate socio-economic impacts of river floods in Europe for the period  
216 1990-2013. Here, the complete procedure is tested using the information collected for the  
217 catastrophic floods of May 2014, which affected several countries in Southeast Europe. In  
218 particular, we focus on the flooding of the Sava River in Bosnia-Herzegovina, Croatia and Serbia.

#### 219 ***3.1 The floods in Southeast Europe in May 2014***

220

221 Exceptionally intense rainfalls from 13 May 2014 onwards following weeks of wet conditions led  
222 to disastrous and wide spread flooding and landslides in South-eastern Europe, in particular  
223 Bosnia-Herzegovina and Serbia. In these two countries, the flood events have been reported to be  
224 the worst for over 200 years. Over 60 people lost their lives and more than a million inhabitants  
225 were estimated to be affected, while the estimated damages and losses exceeded 1.1 billion Euro  
226 for Serbia and 2 billion Euro for Bosnia-Herzegovina (ECMWF, 2014; ICPDR and ISRBC,  
227 2015). Critical flooding was also reported in other countries including Croatia, Romania and  
228 Slovakia. Serbia and Croatia requested and obtained access to the EU Solidarity Fund for major  
229 national disasters (EC 2016).

230 According to the technical report issued by the International Commission for the Protection of  
231 the Danube River and the International Sava River Basin Commission (ICPDR and ISRBC,  
232 2015), the flood events were particularly severe in the middle-lower course of the Sava River and  
233 in several tributaries. The discharge measurements and estimations carried out between 14 and  
234 17 May indicated that the peak flow magnitude exceeded the 500 years return period both in the  
235 Bosna and Kolubara rivers and in part of the Sava River downstream of the confluence with  
236 Bosna. Discharges above 50 years were observed in the Una, Vrbas, Sana and Drina rivers (Figure  
237 3).

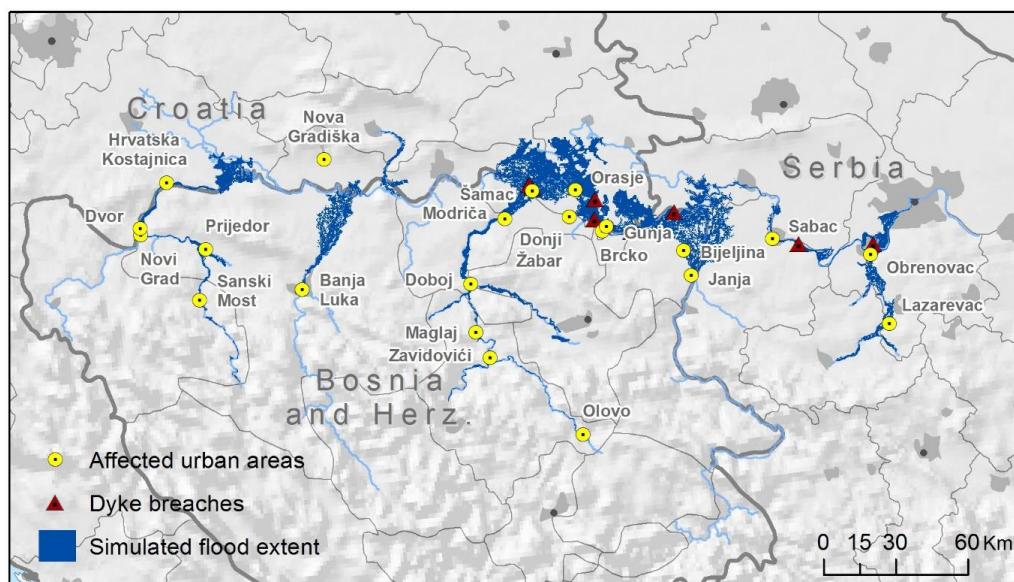


238  
239 *Figure 3. Reconstruction of return period of peak discharges in Sava River basin (source:*  
240 *ICPDR and ISRBC, 2015).*

241  
242 The lower reach of the Sava was less heavily affected because upstream flooding reduced peak  
243 peak discharges and hydraulic operations on the Danube hydraulic structures reduced water levels in  
244 the Danube (ICPDR and ISRBC, 2015). As a result, multiple dyke breaches occurred along the  
245 Sava River, and severe flooding occurred at the confluence of tributaries like Bosna, Drina and  
246 Kolubara due to the extreme discharges (Figure 4). In many areas, dykes were reinforced and  
247 heightened during the flood event to withstand the peak flow; also, additional temporary flood  
248 defences were built to prevent further flooding, and drains were dug to drain flooded areas more  
249 quickly. Other rivers in the area experienced severe flood events, such as the tributaries of the  
250 Danube Velika Morava and Mlava, in Serbia.

251 Table 1 reports a summary of flood impacts at national level for Bosnia-Herzegovina, Croatia and  
252 Serbia, retrieved from different sources.





253  
 254 *Figure 4. Reconstruction of affected urban areas and dyke failure locations along the Sava*  
 255 *River (sources: UNDAC, 2014; ICPDR and ISRBC, 2015). The flood extent of the reference*  
 256 *simulation with the proposed procedure is also shown (see Section 3.2).*  
 257

	Flooded area (km <sup>2</sup> )	Casualties <sup>(1)</sup>	Affected population <sup>(1)</sup>	Evacuated population <sup>(1)</sup>	Economic impact (M€)
Bosnia-Herzegovina	266.3 <sup>(1)</sup> ; 831 <sup>(2)</sup>	25	1.6 million	90000	2040
Croatia	53.5 <sup>(1)</sup> ; 110 <sup>(3)</sup> ; 210 <sup>(4)</sup>	3	38000	15000	300
Serbia	22.4 <sup>(1)</sup> ; 221 <sup>(3)</sup> ; 350 <sup>(5)</sup>	51	1 million	32000	1530 <sup>(1)</sup>

258  
 259 *Table 1. Summary of flood impacts at national level. Figures have been retrieved from the*  
 260 *following sources: 1- ICPDR and ISRBC (2015); 2- Bosnia-Herzegovina Mina Action Center*  
 261 *(BHMAM, Bajic et al 2015); 3- Copernicus EMS Rapid Mapping Service; 4- Wikipedia (2016);*  
 262 *5- GeoSerbia geoportal (2016).*

### 263 3.2 Evaluation of the flood hazard mapping procedure

264  
 265 We considered in our analysis the river network of the Sava River basin, where some of the most  
 266 affected areas are located and for which detailed information is available from various reports.



267 To evaluate the skill of the flood hazard mapping procedure, we used observed flood magnitudes  
268 (Figure 3) to identify the return period of peak discharges and thus select the appropriate flood  
269 maps. In addition, we used the information on flood protection level and dyke failures to select  
270 only those river sections where flooding actually occurred, either because of defence failures or  
271 exceeding discharge. The resulting flood hazard map will be named from now on as “reference  
272 simulation”. Such a procedure excludes the uncertainty due to the hydrological input from the  
273 analysis, focusing on the evaluation of the flood hazard mapping approach alone. In other words,  
274 the test can be seen as an application of the procedure in case of a single, deterministic and  
275 “perfect” forecast. The resulting inundation map is displayed in Figure 4.

276 It is important to note that a margin of uncertainty remains because of the emergency measures  
277 taken during the event. In several river sections of the Sava River, the flood defences were actually  
278 able to withstand discharges well above their design value, thanks to timely emergency measures  
279 such as the heightening and strengthening of dykes. Moreover, the preparation of temporary flood  
280 defences in the floodplains helped to protect some areas which would have been otherwise  
281 flooded. A further issue of the methodology is that, where flood protections are exceeded,  
282 flooding can occur on both river banks, while in case of dyke failure flooding is usually limited  
283 to one side where protection level is lower. This has not been corrected and therefore the results  
284 are affected by this limitation.

285 The flood events in the Sava River have been mapped by several agencies and institutions using  
286 both ground observations and satellite imagery (see UN SPIDER 2014 for a complete list). The  
287 most comprehensive flood maps were developed by the Copernicus Emergency Management  
288 System (EMS) using Sentinel-1 data (EMS, 2014), and by NASA using MODIS Aqua (2014).  
289 For Serbia, the Republic Geodetic authority has acquired and processed further satellite images,  
290 which are available on the geoportal GeoSerbia (2016).

291 Despite this large amount of data sources available, the evaluation of the simulated flood extent  
292 is not straightforward. All the available images have been acquired during the flood recession  
293 (from 19 May onwards), while flood peaks in flooded areas were observed between 15 and 17  
294 May 15 and 17. Therefore, several areas which have been reported as flooded in the available  
295 documentation are not included in the detected flood footprints, which results in a significant  
296 difference between satellite-detected and reported flood extent from ground surveys (see Table  
297 1). On the other hand, EMS satellite maps are designed to produce a low rate of false positive  
298 errors, therefore they can be considered as a “lower limit” for the real flood extent. Finally, it has  
299 to been considered that the available sources of information report for each country different  
300 extents of flooded area, as can be seen in Table 1.

301 In order to take into account these issues, we first compare the total simulated and reported flood  
302 extent, considering all the available reported data. Then, we evaluate the agreement between  
303 satellite-derived and simulated flood extent using the hit ratio  $H$  (Alfieri et al., 2014b). The index  
304 measures the extent of observed flooded area included into estimations and it is defined as:

305  
306

$$H = (Fm \cap Fo) / (Fo) \times 100 \quad (1)$$



307

308 where  $F_m \cap F_o$  is the area correctly predicted as flooded by the model, and  $F_o$  is the total  
309 observed flooded area. As a further element, we compare the number of urban areas (cities, towns  
310 and villages) which were reported as flooded in existing reports.

### 311 *3.2 Evaluation of forecast-based flood maps*

312

313 To evaluate the overall performance of forecast-based flood mapping, we considered the EFAS  
314 forecasts issued on 12 and 13 May for the Sava river basin, that is, immediately before the  
315 occurrence of first flood events on 14 May. We first applied the procedure described in Section  
316 2.3 to derive peak discharges and the estimated return period using the median of the EFAS  
317 ensemble forecasts. To provide an indication of the possible range of risk scenarios, we produced  
318 additional flood hazard maps with the same procedure considering the 25 and 75 percentiles of  
319 discharge.

320 The forecast-based flood hazard maps are evaluated against the reference simulation, comparing  
321 the river sectors and the urban areas (or municipalities) at risk of flooding. Note that no direct  
322 comparison against observation-based flood maps has been carried out, because forecast-based  
323 maps cannot account for defence failures or strengthening.

### 324 *3.3 Evaluation of the flood risk assessment*

325

326 Inundation maps derived from the reference simulation and flood forecasts have been used to  
327 compute the flood impacts in terms of number of affected people, affected major towns and cities,  
328 and economic damage.

329 The results are compared with the available impact estimations both at national and local level.  
330 For Serbia and Bosnia-Herzegovina, the national figures reported in Table 1 are referred to the  
331 total impact given by river floods, landslides and pluvial floods, therefore they cannot be directly  
332 compared with methodology results. As such, the comparison has been done only for Croatia and  
333 for a number of municipalities (e.g. Obrenovac in Serbia) where impacts can be attributed to river  
334 flooding alone.

335 The figures of affected population simulated with the observation-based flood scenario are also  
336 useful to test the reliability of the population map used as exposure dataset. Similarly, damage  
337 estimations coming from the observation-based scenario provide an indication of the reliability  
338 of depth-damage curves for the study area.

339 As done for the flood hazard maps, forecast-based risk estimations are evaluated against the  
340 observation-based estimations, comparing both population and damage figures. Note that other  
341 variables produced by the operational procedure (e.g. roads affected, flooded urban and  
342 agricultural areas) could not be tested due to the lack of observed data and therefore are not  
343 discussed here. To add a further term of comparison, affected population has been computed using  
344 Copernicus-EMS flood footprints.



345 **4) Results and discussions**

346

347 The results of the validation exercise are shown and discussed separately for each component of  
 348 the procedure.

349 **4.1 Flood hazard mapping**

350

351 Table 3 reports the observed flood extent data from different sources and the simulated extent  
 352 derived from the reference simulation (i.e. the mapping procedure applied on discharge  
 353 observations). Table 4 reports the scores of the hit ratio H for a number of flooded river sections,  
 354 together with a comparison of towns flooded according to simulations and observation.  
 355

Country	Flood extent (km <sup>2</sup> )			
	Simulated	Satellite	Reported by ICPDR-ISRBC	Reported (other sources)
<b>Bosnia - Herzegovina</b>	995	339	266.3 <sup>(1)</sup>	831 <sup>(2)</sup>
<b>Croatia</b>	919 (319)	110	53.5 <sup>(1)</sup>	>210 <sup>(3)</sup>
<b>Serbia</b>	582	221	22.4 <sup>(1)</sup>	>350 <sup>(4)</sup>

356

357 *Table 3. Comparison of observed and simulated flood extent data at country scale. Satellite*  
 358 *flood extent is referred to Copernicus EMS maps. The value between parentheses for Croatia is*  
 359 *based on a modified simulation, as explained in the text. Reported flood extent has been*  
 360 *retrieved from the following sources: 1- ICPDR and ISRBC (2015); 2- BHMACH(Bajic et al*  
 361 *2015); 3- Wikipedia (2016); 4 – GeoSerbia geoportal (2016).*  
 362

Affected areas	Hit ratio	EMS flooded area (km <sup>2</sup> )	Affected towns and cities
Bosna River	90.6%	58.46	Maglaj, Doboj, Modriča
Sava River between confluences with Bosna and Drina	63.9%	134.76	Orašje, Šamac, Donji Žabar, Breko, Gunja, (Zupanja), Bijeljina
Sava River between confluences with Drina and Kolubara	83.7%	405.43	Sabac, Obrenovac, Lazarevac
Total	79.9%	598.65	

363 *Table 4. Scores of the hit ratio H for a number of flooded river sections, and affected towns and*  
 364 *cities. Names between parentheses refer to towns and cities wrongly predicted as flooded,*  
 365 *otherwise towns and cities have been correctly predicted as flooded.*  
 366



367 As expected, the simulated flood extent is significantly larger in all the cases than the satellite  
368 extent (see Table 3), given the delay between flood peaking time and time of image acquisition  
369 mentioned in Section 3.2. For Serbia in particular the flooded area detected from Copernicus and  
370 GeoSerbia maps are both smaller than the simulation. Also, flood extent indicated in the ICPDR  
371 and ISRBC report is consistently lower than values from both simulated and satellite maps.  
372 For Bosnia-Herzegovina, the simulated value is close to the reported flood extent published in a  
373 report by Bajic et al. (2015). For Croatia, the flood mapping methodology is largely  
374 overestimating both the satellite-based and reported flood extents. The main reason is that  
375 flooding on the left side of Sava was limited due to the reinforcing of river dykes in the area close  
376 to the city of Zupanja, which could contain the reported 500 years return period discharge despite  
377 having been designed for a 1 in 100 year event. In fact, all the left bank of Sava in this area was  
378 reported as areas at risk in case of a failure of flood defences, and only the emergency measures  
379 taken prevented more severe flooding (ISRBC, 2014). We performed an additional flood  
380 simulation excluding any failure on the river left bank between the Bosna confluence and  
381 Zupanja, and in this case we found a total flood extent of 319 km<sup>2</sup>. Although this value is larger  
382 than for satellite maps, it is close to the extent reported by other sources.  
383 Regarding Table 4, the scores of the H index indicate that the mapping procedure can correctly  
384 detect most of the flooded areas, although with the partial exception of the lower Sava area. In  
385 particular, the great majority of towns reported to have been flooded are correctly detected by the  
386 simulations, with only few false alarms (e.g. the already mentioned Zupanja).  
387 When looking at the results it's important to keep in mind the limitations of the procedure. As  
388 mentioned in Section 2.3, the mapping procedure is able to reproduce only maximum flood  
389 depths, and the dynamic of the flood event is not taken into account. This means that processes  
390 like flood wave attenuation due to inundation occurring upstream cannot be simulated, and  
391 possible flood mitigation measures taken during the event are not considered as well.  
392 Furthermore, due to the DEM coarse resolution, flood simulations do not include small scale  
393 topographic features like minor river channels, dykes and road embankments.

#### 394 *4.2 Flood risk assessment*

395  
396 Tables 5 and 6 show a summary of the simulated flood impacts on population (based on the  
397 reference simulation), compared with estimates both at local scale and aggregated at national  
398 scale. Note that we compare simulated population impacts with figures of evacuated population  
399 because the reported estimates of affected population included also people affected by pluvial  
400 floods and landslides, as well as indirect effects like energy shortage and road cuts. On the other  
401 hand, it is important to remember that the figures of evacuated population are not equivalent to  
402 directly affected population (i.e. whose houses were actually flooded). In some areas, evacuation  
403 was taken as a precautionary measure, even if flooding did not eventually occur.

404



Country	Evacuated population (reported)	Affected population (satellite)	Affected population (simulated)
Bosnia-Herzegovina	90.000	51.010	215.200
Croatia	27.255	5.758	57.000
Serbia	32.000	13.699	29.800

405 *Table 5. Comparison of evacuated population and affected population estimated from satellite*  
 406 *and simulations in Bosnia-Herzegovina, Croatia and Serbia (source: ICPDR and ISRBC,*  
 407 *2015).*  
 408

Administrative area	Country	Evacuated population (reported)	Affected population (estimated)
Obrenovac municipality	Serbia	> 25000	17600
Brod-Posavina county	Croatia	13700	12800
Osijek-Baranja county	Croatia	200	1300
Sisak-Moslavina county	Croatia	2400	3300
Požega-Slavonija county	Croatia	2300	1500
Vukovar-Srijem county	Croatia	8700	39200

409  
 410 *Table 6. Comparison of evacuated population (reported) and affected population (simulated) in*  
 411 *administrative areas in Croatia and Serbia (source: ICPDR and ISRBC, 2015; Wikipedia,*  
 412 *2016)*  
 413

414 As can be seen, results from the reference simulation match well figures reported for all the  
 415 flooded counties of Croatia except for the Vukovar-Srijem County. This is due to the  
 416 overestimation of flooded areas due to the emergency measures mentioned in Section 4.1. If these  
 417 are taken into account and dyke failures are not included in this county, the affected population  
 418 is reduced to 8600 people, extremely close to the reported figure. Some underestimation can be  
 419 observed for Obrenovac municipality but the estimated figures still depict a major impact on the  
 420 city. A possible reason is that the flood simulations are less reliable for urban areas, as the  
 421 elevation data from SRTM is known to be less accurate in urban and densely vegetated areas  
 422 (Sampson et al., 2015). It is worth noting that simulated and reported figures for affected people  
 423 compare much better than for flood extent, which supports the hypothesis of a general  
 424 underestimation of flood extent from satellite images.

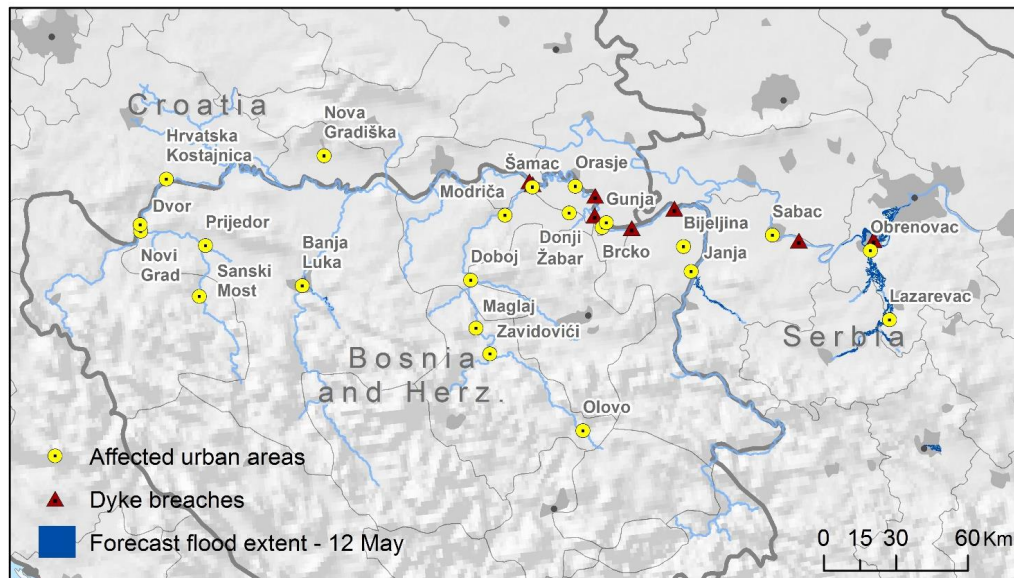
425 For flood impacts related to monetary damage, the simulations for Croatia report a total damage  
 426 of 653 M€, against a reported estimate of 298 M€. However, if the already mentioned  
 427 overestimation of flooded areas is considered, then the estimate decreases to 190 M€. As  
 428 mentioned in Section 3.3, damage figures Serbia and Bosnia-Herzegovina could not be used  
 429 because available estimates aggregate damages from landslides and river and pluvial flooding.



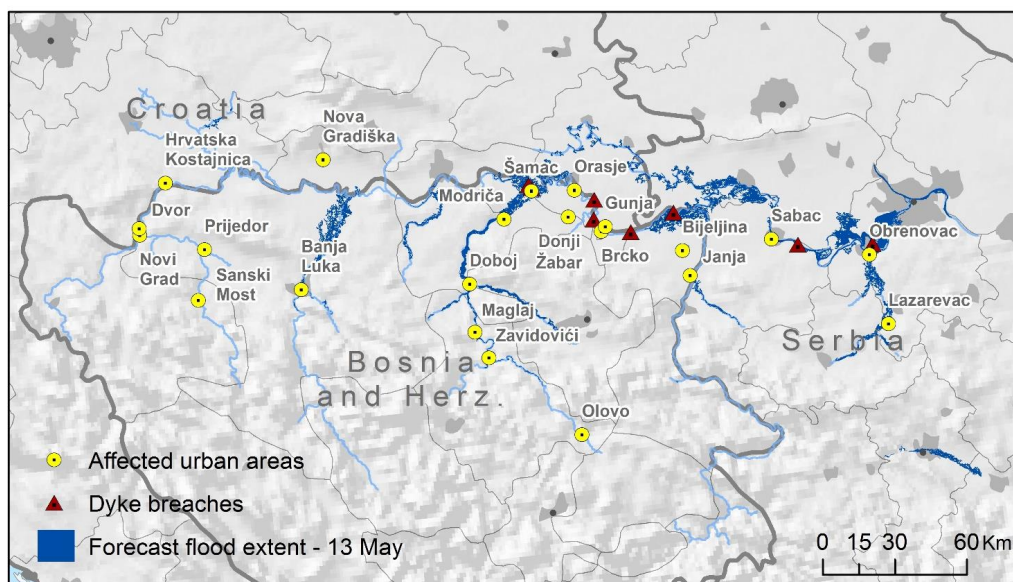
430 The observed underestimation can be explained considering that the damage curves applied have  
431 not yet been calibrated for Bosnia-Herzegovina, Croatia and Serbia. On this point, previous  
432 applications in countries where established damage curves were available (e.g. Germany) led to  
433 results well in line with observations (Jongman et al., 2012; Alfieri et al., 2016). Also, estimated  
434 damages include only direct damage to buildings, while infrastructural damage is only partially  
435 accounted for (e.g. damage to the dyke system).

#### 436 4.3 EFAS forecasts

437  
438 Figures 5 and 6 show the inundation maps derived using the median of ensemble streamflow  
439 forecasts issued on 12 and 13 May (that is, the standard procedure adopted for the operational  
440 procedure). In addition, Table 7 illustrates the outcomes of impact forecasts, compared to impacts  
441 obtained from the reference simulation. For 12 May, we considered predicted maximum  
442 streamflow values based on the 25<sup>th</sup>, 50<sup>th</sup> and 75<sup>th</sup> percentiles of the ensemble forecast. For 13  
443 May only the 50<sup>th</sup> percentile is considered. All of estimations are computed taking into account  
444 local flood protection levels.



445  
446 *Figure 5. Simulated flood extent based on 12 May forecast, with location of reported flooded*  
447 *urban areas and dyke failures.*



448  
 449 *Figure 6. Simulated flood extent based on 13 May forecast, with location of reported flooded*  
 450 *urban areas and dyke failures.*

451

Country	12 May - 25 perc	12 May 12 -50 perc	12 May - 75 perc	13 May - 50 perc	Reference
flood extent (km <sup>2</sup> )					
Bosnia-Herzegovina	0	5	196	509	995
Croatia	0	0	100	159	919
Serbia	91	187	385	658	582
affected population					
Bosnia-Herzegovina	0	5,225	20,458	100,665	215,176
Croatia	0	0	3,598	4,924	57,053
Serbia	2,793	6,012	15,120	27,732	29,758
economic damage (million €)					
Bosnia-Herzegovina	0	10	36	254	378
Croatia	0	0	41	54	653
Serbia	14	31	92	203	141

452

453

454

455

456

*Table 7. Comparison of forecasted flood impacts with the reference impact estimation.*

The simulated flood maps and the values displayed in Table 7 show that, while forecasts for 12 May are significantly far from the observations, the performance greatly improves after one single





457 day, when predicted impacts are very similar to the reference simulation for Serbia, even though  
458 for Bosnia- Herzegovina and especially Croatia there is still a significant underestimation.  
459 Nevertheless, the order of magnitude is already indicating a major flood risk for the predicted  
460 events, meaning that emergency responders could have used this estimation to plan and  
461 implement countermeasures, and monitor the situation. A further important result is that the  
462 location of forecasted flooded areas is mostly consistent with the reference simulation shown in  
463 Figure 3, with several urban areas already at risk of flooding in the map based on 13 May forecast  
464 (Figure 6).

465 Regarding the prediction based on 12 May forecast, it is worth noting that the use of 75<sup>th</sup> percentile  
466 results in estimations closer to the reference simulation (Table 7). Again, this is an important  
467 piece of information because it provides emergency responders with an early indication of the  
468 possible severe consequences of the upcoming flood.  
469

## 470 *5) Conclusions and next developments*

471

472 This paper presents the first application of an impact forecasting procedure which is fully  
473 integrated within a continental scale flood early warning system. The procedure has been  
474 thoroughly tested in all its components, and the results demonstrate the potential of the proposed  
475 approach. Comparison of reported and simulated flooded areas suggests that the methodology  
476 enables to identify areas at risk well in advance, which could help the planning of timely response  
477 measures (e.g. dyke strengthening, temporary road closure).

478 The methodology provided acceptable estimates of affected population, thus providing valuable  
479 information for the implementation of evacuation measures. Damage estimations are in the same  
480 order of magnitude of observed figures, albeit with a general underestimation. It should be  
481 considered, however, that the damage curves used for Bosnia-Herzegovina, Croatia and Serbia  
482 are curves that have been derived for other European countries rescaled to reflect local asset  
483 values. Further applications will allow to improve estimations by calibrating damage curves in  
484 different contexts and more countries.

485 When evaluating the outcomes, it is important to remember that, even in case of a risk assessment  
486 based on “perfect” forecasts and modelling, simulated impacts will always be different from  
487 actual impacts. As we have shown in the test case of the floods in the Sava River basin,  
488 unexpected defence failures can occur for flow magnitudes lower than the design level, thus  
489 increasing flood impacts. On the other hand, flood defences might be able to withstand greater  
490 discharges than the design level, and emergency measures can improve the strength of flood  
491 defences or creating new temporary structures. Finally, evaluating forecasted impacts is still  
492 complicated by the lack of standardized reporting of flood impacts, meaning that reported flood  
493 extents and damages can strongly deviate from the true extents and damages (as observed in the  
494 test case from the differences between the satellite and reported extents). As such, forecast-based  
495 risk assessment should be regarded as a flood scenario that can provide valuable information for



496 local, national and international authorities, complementing the standard information provided by  
497 flood early warning systems.

498 Since September 2016, the procedure is running in testing mode within the EFAS modelling chain  
499 and will be fully operational by the beginning of 2017. Besides the version currently in use and  
500 described in this paper, further modifications and alternative approaches for hazard mapping and  
501 risk assessment will be tested in the near future.

502 Currently, inundation forecasting is computed using the median of daily ensemble streamflow  
503 forecasts, but in principle the methodology can easily be adapted to produce additional flood  
504 scenarios considering different ensemble percentiles, thus taking into account less probable but  
505 potentially more severe flood scenarios (see the application described this paper). Alternatively,  
506 the uncertainty of meteorological predictions could be represented using probabilistic maps of  
507 flood extent as proposed by Di Baldassarre et al. (2010). The influence of lead time on flood  
508 predictions could also be assessed, for instance by setting a criterion based on forecasts  
509 persistence over a period to trigger the release of impact forecasts. All these alternatives will be  
510 tested in collaboration with the community of the EFAS users, to maximize the value of the  
511 information provided and avoid information overload which can be difficult to manage in  
512 emergency situations.

513 A further promising application is the possibility of using inundation forecast to activate rapid  
514 flood mapping from satellites, exploiting the Copernicus Emergency Mapping Service of the  
515 European Commission.

516 Finally, the proposed procedure will also be incorporated into the Global Flood Awareness  
517 System (GloFAS), which would allow to establish a near-real time flood risk alert system at global  
518 scale.

519

## 520 *Acknowledgements*

521

522 This work has been partially funded by the COPERNICUS programme and an administrative  
523 arrangement with the Directorate General Humanitarian Aid and Civil Protection (DG ECHO) of  
524 the European Commission.

525 The authors would like to thank Jutta Thielen for her valuable suggestions on an early version of  
526 the manuscript.

527

## 528 *Bibliography*

529

530 Alfieri L., Pappenberger F., Wetterhall F., Haiden T., Richardson D., Salamon P., 2014a.  
531 Evaluation of ensemble streamflow predictions in Europe, *Journal of Hydrology*, 517, 913-922

532 Alfieri, L., Salamon, P., Bianchi, A., Neal, J., Bates, P.D., Feyen, L., 2014b. Advances in pan-  
533 European flood hazard mapping, *Hydrol. Process.*, 28 (18), 4928-4937, doi:10.1002/hyp.9947.



- 534 Alfieri L., Feyen L., Dottori F., Bianchi A., 2015. Ensemble flood risk assessment in Europe  
535 under high end climate scenarios. *Global Environmental Change* 35, 199–212.
- 536 Alfieri, L., Feyen, L., Salamon, P., Thielen, J., Bianchi, A., Dottori, F., and Burek, P.:  
537 Modelling the socio-economic impact of river floods in Europe, *Nat. Hazards Earth Syst. Sci.*,  
538 16, 1401-1411, doi:10.5194/nhess-16-1401-2016, 2016.
- 539 Bates P.D., Horritt M.S., and Fewtrell T.J. (2010). A simple inertial formulation of the  
540 shallow water equations for efficient two-dimensional flood inundation modelling. *Journal of*  
541 *Hydrology*, 387, 33–45.
- 542 Batista e Silva F., Gallego J., and Lavalle C. (2013). A high-resolution population grid map  
543 for Europe. *Journal of Maps*, 9 (1), 16-28.
- 544 Burek, P., Knijff van der, J., Roo de, A., 2013. LISFLOOD, Distributed Water Balance and  
545 Flood Simulation Model Revised User Manual 2013. Publications Office, Luxembourg.
- 546 Cloke, H., Pappenberger, F., Thielen, J. and Thiemig, V. (2013) Operational European Flood  
547 Forecasting, in *Environmental Modelling: Finding Simplicity in Complexity*, Second Edition (eds  
548 J. Wainwright and M. Mulligan), John Wiley & Sons, Ltd, Chichester, UK. doi:  
549 10.1002/9781118351475.ch25.
- 550 Copernicus Emergency Management Service - Mapping. Institute for the Protection and  
551 Security of the Citizen (IPSC), European Commission, Joint Research Centre (JRC). Accessed  
552 November 12, 2014. <http://emergency.copernicus.eu/>.
- 553 Di Baldassarre G, Schumann G, Bates PD, Freer JE, and Beven KJ. (2010). Floodplain  
554 mapping: a critical discussion of deterministic and probabilistic approaches. *Hydrological*  
555 *Sciences Journal*, 55 (3), 364–376.
- 556 Dottori F., Salamon P., Kalas M., Bianchi A., Thielen J., Feyen L., 2015. A near real-time  
557 procedure for flood hazard mapping and risk assessment in Europe. 36th IAHR World Congress  
558 28 June – 3 July, The Hague, the Netherlands.
- 559 EC, 2016. List of EU Solidarity Fund Interventions since 2002,  
560 [http://ec.europa.eu/regional\\_policy/sources/thefunds/doc/interventions\\_since\\_2002.pdf](http://ec.europa.eu/regional_policy/sources/thefunds/doc/interventions_since_2002.pdf)  
561 (accessed 15-9-2016).
- 562 EC, 2007. Directive 2007/60/EC of the European Parliament and of the Council on the  
563 assessment and management of flood risks. *Official Journal of the European Communities*,  
564 Brussels, <http://eur-lex.europa.eu/legal-content/EN/TXT/?uri=CELEX%3A32007L0060>  
565 (accessed 21-10-2016).
- 566 ECMWF, 2014. EFAS Bulletin April – May 2014. Available at [https://www.efas.eu/efas-](https://www.efas.eu/efas-bulletins/1801-efas-bulletin-april-may-2014-issue-20143.html)  
567 [bulletins/1801-efas-bulletin-april-may-2014-issue-20143.html](https://www.efas.eu/efas-bulletins/1801-efas-bulletin-april-may-2014-issue-20143.html) (accessed October 2015).
- 568 Emerton, R., Stephens, E.M., Pappenberger, F., Pagano, T.C., Weerts, A.H., Wood, A.W.,  
569 Salamon, P., Brown, J.D., Hjerdt, N., Donnelly, C., Baugh, C.A., Cloke, H.L., 2016. Continental  
570 and global scale flood forecasting systems. *WIREs Water* 2016 (3) 391–418,  
571 doi:10.1002/wat2.1137.
- 572 Geoportals GeoSerbia, <http://www.geosrbija.rs/> (accessed 21-10-2016).



- 573 Huizinga H. J. (2007). Flood damage functions for EU member states, HKV Consultants,  
574 Implemented in the framework of the contract #382442-F1SC awarded by the European  
575 Commission – Joint Research Centre.
- 576 Jongman B., Kreibich H., Apel H., Barredo J.I., Bates P.D., Feyen L., Gericke A., Neal J.,  
577 Aerts J.C.J.H and Ward P.J (2012). Comparative flood damage model assessment: towards a  
578 European approach. *Natural Hazards and Earth System Sciences*. 12, 3733–3752.
- 579 Jongman, B., Hochrainer-Stigler, S., Feyen, L., Aerts, J.C.J.H., Mechler, R., Botzen, W.J.W.,  
580 Bouwer, L.M., Pflug, G., Rojas, R., Ward, P.J., 2014. Increasing stress on disaster-risk finance  
581 due to large floods. *Nat. Clim. Change* 4, 264–268. doi:<http://dx.doi.org/10.1038/nclimate2124>.
- 582 ICPDR – International Commission for the Protection of the Danube River and ISRBC –  
583 International Sava River Basin Commission 2015. Floods in May 2014 in the Sava River Basin.  
584 [https://www.icpdr.org/main/sites/default/files/nodes/documents/sava\\_floods\\_report.pdf](https://www.icpdr.org/main/sites/default/files/nodes/documents/sava_floods_report.pdf)  
585 (accessed 11-10-2015).
- 586 Marín Herrera, M., Batista e Silva, F., Bianchi, A., Barranco, R. and Lavalle, C., 2015. A  
587 geographical database of infrastructures in Europe. JRC Technical Report, JRC99274.
- 588 Pappenberger F., Thielen J., and Del Medico M. (2011). The impact of weather forecast  
589 improvements on large scale hydrology: analysing a decade of forecasts of the European Flood  
590 Alert System. *Hydrological Processes*, 25, 1091–1113. <http://dx.doi.org/10.1002/hyp.7772>.
- 591 Pappenberger F., Cloke, H. L., Parker, D.J., Wetterhall, F., Richardson, D.S, Thielen, J., 2015.  
592 The monetary benefit of early flood warnings in Europe. *Environmental Science & Policy* 51,  
593 278–291.
- 594 Rojas, R., Feyen, L., Watkiss, P., 2013. Climate change and river floods in the European  
595 Union: socio-economic consequences and the costs and benefits of adaptation. *Glob. Environ.*  
596 *Change* 23, 1737–1751. doi:<http://dx.doi.org/10.1016/j.gloenvcha.2013.08.006>.
- 597 Rossi, L., Rudari, R., and the RASOR Team. RASOR Project: Rapid Analysis and  
598 Spatialisation of Risk, from Hazard to Risk using EO data. *Geophysical Research Abstracts* Vol.  
599 18, EGU2016-15073.
- 600 Saint-Martin, C., Fouchier, C., Douvinet, J., Javelle, P., Vinet, F., 2016. Contribution of an  
601 exposure indicator to better anticipate damages with the AIGA flood warning method: a case  
602 study in the South of France. *Geophysical Research Abstracts* Vol. 18, EGU2016-10305-4.
- 603 Sampson, C.C., Smith, A.M, Bates, P.D., Neal, J.C., Alfieri, L., Freer, J.E., 2015. A High  
604 Resolution Global Flood Hazard Model. Accepted article in *Water Resour. Res.*, doi:  
605 [10.1002/2015WR016954](https://doi.org/10.1002/2015WR016954).
- 606 Schulz, A., Kiesel, J., Kling, H., Preishuber M., Petersen G., 2015. An online system for rapid  
607 and simultaneous flood mapping scenario simulations - the Zambezi FloodDSS. *Geophysical*  
608 *Research Abstracts* Vol. 17, EGU2015-6876. Thielen J., Bartholmes J., Ramos M.H., and De Roo  
609 A. (2009). The European flood alert system – part 1: concept and development. *Hydrology and*  
610 *Earth System Sciences* 13, 125–140.
- 611 UNDAC - United Nations Disaster Assessment and Coordination Team, 2014. Mission to  
612 Serbia – Floods 18-31 May 2014, end of mission report.



- 613 Van der Knijff, J.M., Younis, J., de Roo, A.P.J., 2010. LISFLOOD: a GIS-based distributed  
614 model for river basin scale water balance and flood simulation. *Int. J. Geogr. Inf. Sci.* 24, 189–  
615 212.
- 616 Ward, P., Coughlan de Perez, E., Dottori, F., Jongman, B., Luo T., Safaie S., Uhlemann-Elmer  
617 S., 2016. The need for mapping, modelling and predicting flood hazard and risk at the global  
618 scale. In publication in: *Global Flood Hazard: Applications in modeling, mapping and forecasting*  
619 (Eds. Guy Schumann, Paul Bates, Giuseppe Aronica and Heiko Apel).
- 620 Wikipedia. *Poplave u istočnoj Hrvatskoj u svibnju 2014* (accessed 21-10-2016).